Comp. & Maths. with Appls. Vol. 10, No. 3, pp. 291–304, 1984
Printed in the U.S.A.

0097-4943/84 $3.00 + .00

MIXED CONVECTION FLOW OF A MICROPOLAR FLUID FROM AN ISOTHERMAL VERTICAL PLATE

S. K. JENA and M. N. MATHUR
Department of Mathematics, Indian Institute of Technology, Powai, Bombay 400076, India

(*Received October* 1983)

Communicated by Ervin Y. Rodin

Abstract—Laminar mixed convection boundary layer flow of a micropolar fluid from an isothermal vertical flat plate has been considered. This problem does not admit similarity solutions and has been solved numerically by using a finite-difference technique in a finite domain. Velocity, microrotation and temperature fields have been computed and shown graphically from pure forced convection to moderately large free convection flows. The skin-friction and the rate of heat transfer parameters on the plate have been tabulated. It is found that velocity increases and temperature decreases with the heating of the fluid while these results reverse for the cooling of the fluid. It is observed that the microrotation is very sensitive to the changes in the values of Grashof number when fluid is being heated by the free convection current while it is rather insensitive when fluid is being cooled by the free convection current. Furthermore, the results have been compared with the results of the corresponding flow of a Newtonian fluid.

1. INTRODUCTION

Thermal buoyancy effects on forced convective heat transfer over a surface may become important when the flow velocity is relatively small and the temperature difference between the surface and the ambient fluid is large. The thermal buoyancy force effects on heat transfer characteristics of forced convection have been studied fairly extensively for various flow configurations, particularly the forced flow along a vertical surface. Several investigators[1–4] have reported on the theoretical work in the field of heat transfer from a heated vertical plate with combination of free- and forced-convection flow for a Newtonian fluid. However, there is no such work available in the literature for fluids which are a mixture of heterogeneous means such as liquid crystals, polymers, polycrystalline aggregate, granular media, ferro-liquid etc., which is more realistic and important from the technological point of view. The occurrence of bar like elements or polymeric additives rotating in fluids has been found to affect the heat exchange processes significantly[5]. For the realistic description of the flow of fluids such as fluids with polymeric additives etc., the classical continuum mechanics cannot be used because it regards them as single continuum. In order to describe adequately the nature of such substances, it seems to be necessary to assume that the material consists of more than one constituent. The theoretical study of this system of fluids has been very useful in understanding such phenomena as sedimentation, fluidization, combustion, environmental pollution and so on. It is interesting to note that several theories, e.g. polar fluids, dipolar fluids, couple stress fluids, anisotropic fluids, asymmetric hydromechanics etc., exist to describe the flow behaviour of such rheologically complex fluids. However, it has been demonstrated by Ariman *et al.*[6] that for linear viscous and isotropic fluids all these theories can be considered as equivalent to micropolar fluid theory[7] proposed by Eringen. Moreover, the micropolar fluid model is more suitable because the microcontinuum approach describes the microscopic events, microrotation and shape and size of the suspended particles. A detailed and rigorous theoretical approach of modern phase of the continuum theory of mixture can be found in the papers by Eringen[7–9].

The literature on free convection flow of micropolar fluids is small but growing. The problems of convective heat transfer of micropolar fluids in a vertical channel and in a horizontal parallel plate channel have been considered by Balaram and Sastry[10] and Maiti[11] respectively. Sastry and Maiti[12] have studied the problem of free and forced convective heat transfer in a micropolar fluid in an annulus of two vertical pipes. In all

these studies[10–12] boundary layer concepts in convective flow have not been taken into account. Very recently, Jena and Mathur[13] have studied the free convection in the boundary layer flow of a micropolar fluid past a non-isothermal vertical flat plate.

The boundary layer equations for the combined free- and forced-convection flow of a micropolar fluid over a vertical flat plate do not admit similarity solutions, as it was in the case of only free convection[13]. The solutions to these boundary layer equations may be obtained through the application of the finite-difference technique. Using this procedure, it is possible to determine the velocity and temperature fields in the boundary layer for a wide class of problems as a function of the plate temperature as well as thermal properties of the plate and fluid. But, when finite-difference methods are employed for the numerical solution of the problems concerned with regions of infinite extent in one or more directions, there are two main difficulties to be faced, viz., the satisfaction of boundary conditions at infinity and the representation of an infinite interval with a finite number of grid points. To overcome these difficulties, Sills[14] has proposed three types of transformations. The one most suited for the application of finite-difference schemes is to map the infinite field into a finite one by introducing a co-ordinate transformation. Sills[14] has presented transformations which map one or both of the intervals $(0, \infty)$ and $(-\infty, \infty)$ into finite intervals along with an illustration of their application to flow problems. The asymptotic nature of these transformations allows the straightforward application of the boundary conditions at infinity and at the same time concentrating the grid points in the desired region and eliminating the necessity of searching for the effective boundary layer edge through additional iteration.

In the present paper, we have studied the laminar boundary layer free convection in a micropolar fluid from an isothermal vertical flat plate placed in an external uniform flow. Such a flow is termed as mixed or combined free- and forced-convection flow. The equations governing the flow are transformed into new co-ordinates with a finite domain using the transformation given by Sills[14]. These equations are then decoupled and each equation is solved for a single dependent variable using finite-difference technique. The results have been obtained from pure forced convection to moderately large free convection flow.

2. FORMULATION OF THE PROBLEM

We shall assume that the x-axis is placed in the plane of the plate in the direction of flow, the y-axis being at right angles to it and to the flow, with the origin at the leading edge. The equations governing the steady laminar boundary layer flow of an incompressible micropolar fluid past a vertical flat plate are

Continuity

$$\frac{\partial u}{\partial x} + \frac{\partial v}{\partial y} = 0. \tag{2.1}$$

Momentum

$$\rho\left(u\frac{\partial u}{\partial x} + v\frac{\partial u}{\partial y}\right) = (\mu_v + K_v)\frac{\partial^2 u}{\partial y^2} + K_v\frac{\partial v}{\partial y} + \rho g\beta(T - T_\infty). \tag{2.2}$$

Moment of momentum

$$\rho j\left(u\frac{\partial v}{\partial x} + v\frac{\partial v}{\partial y}\right) = \gamma_v\frac{\partial^2 v}{\partial y^2} - K_v\left(\frac{\partial u}{\partial y} + 2v\right). \tag{2.3}$$

Energy

$$\rho c_v\left(u\frac{\partial T}{\partial x} + v\frac{\partial T}{\partial y}\right) = k_c\frac{\partial^2 T}{\partial y^2}, \tag{2.4}$$

where u, v = components of velocity along and normal to the vertical flat plate; v = component of microrotation whose direction of rotation is in the xy-plane; ρ, T = density and temperature of the fluid; μ_v, K_v, γ_v = viscosity, vortex viscosity and spin-gradient viscosity; j, k_c = micro-inertia density and thermal conductivity; g, β, c_v = acceleration due to gravity, coefficient of thermal expansion and specific heat of the fluid at constant volume.

The details of the derivation of the boundary layer equations (2.1)–(2.4) are available in [15, 16].

In the present investigation, the effects of viscous dissipation and the micropolar heat conduction have been neglected. Similar consideration has been made by several investigators [16–18]. This is indeed a permissible simplification in this flow problem since the heat transfer due to free convection results in low velocities and is normally associated with large temperature differences. It has also been recently shown by Mathur *et al.* [16] that viscous dissipation and the micropolar heat conduction have very little effect on the temperature field and the rate of heat transfer for the flow of an incompressible micropolar fluid past a circular cylinder placed in such a way that its axis is normal to the oncoming free stream.

The boundary conditions for equations (2.1)–(2.4) are

$$\begin{aligned} y = 0&: u = 0,\ v = 0,\ v = 0,\ T = T_w, \\ y \to \infty&: u \to U_\infty,\ v \to 0,\ T \to T_\infty, \end{aligned} \tag{2.5}$$

where T_w, U_∞, T_∞ are respectively the constant temperature of the plate, free stream velocity and free stream temperature.

This is to be noted that the various material parameters occurring in the theory of micropolar fluids satisfy a number of inequalities which are necessary and sufficient to ensure that the rate of dissipation of energy should be non-negative. These inequalities have been discussed in detail by Eringen [7–9].

We introduce the following dimensionless quantities in equations (2.1)–(2.4) and boundary conditions (2.5):

$$\begin{aligned} &x^* = \frac{x}{(\mu_v/\rho U_\infty)}, \quad y^* = \frac{y}{(\mu_v/\rho U_\infty)}, \quad u^* = \frac{u}{U_\infty}, \\ &v^* = \frac{v}{U_\infty}, \quad v^* = \frac{v}{(\rho U_\infty{}^2/\mu_v)}, \quad \theta = \frac{T - T_\infty}{T_w - T_\infty}, \\ &N_1 = \frac{K_v}{\mu_v}, \quad N_2 = \frac{j}{(\mu_v/\rho U_\infty)^2}, \quad N_3 = \frac{\gamma_v}{\mu_v(\mu_v/\rho U_\infty)^2}, \\ &\mathrm{Pr} = \frac{\mu_v C_v}{k_c}, \quad \mathrm{Gr} = \frac{g\beta(T_w - T_\infty)\mu_v}{\rho U_\infty{}^3}, \end{aligned} \tag{2.6}$$

where Gr is the Grashof number and Pr is the Prandtl number. The parameters N_1, N_2 and N_3, respectively, characterise the vortex viscosity, micro-inertia density and spin-gradient viscosity.

The equations (2.1)–(2.4) in non-dimensional form, after dropping the asterisks, become

$$\frac{\partial u}{\partial x} + \frac{\partial v}{\partial y} = 0 \tag{2.7}$$

$$u\frac{\partial u}{\partial x} + v\frac{\partial u}{\partial y} = (1 + N_1)\frac{\partial^2 u}{\partial y^2} + N_1\frac{\partial v}{\partial y} + \mathrm{Gr}\,\theta \tag{2.8}$$

$$N_2\left(u\frac{\partial v}{\partial x} + v\frac{\partial v}{\partial y}\right) = N_3\frac{\partial^2 v}{\partial y^2} - N_1\left(\frac{\partial u}{\partial y} + 2v\right) \tag{2.9}$$

$$u\frac{\partial\theta}{\partial x}+v\frac{\partial\theta}{\partial y}=\frac{1}{\mathrm{Pr}}\frac{\partial^2\theta}{\partial y^2}. \tag{2.10}$$

The corresponding boundary conditions are

$$\begin{aligned} &y=0\text{: } u=0,\ v=0,\ v=0,\ \theta=1,\\ &y\to\infty\text{: } u\to1,\ v\to0,\ \theta\to0. \end{aligned} \tag{2.11}$$

We now introduce the following transformations:

$$\eta(x,y)=\frac{y}{\sqrt{2\xi}},\quad \xi(x)=x. \tag{2.12}$$

Further, we write

$$\psi=\sqrt{2\xi}f(\xi,\eta),\quad v=\frac{1}{\sqrt{2\xi}}G(\xi,\eta), \tag{2.13}$$

where $\psi(x,y)$ is the stream function such that

$$u=\frac{\partial\psi}{\partial y}\quad\text{and}\quad v=-\frac{\partial\psi}{\partial x}.$$

Making use of (2.12) and (2.13), and denoting

$$u=F=\frac{\partial f}{\partial\eta},\quad V=-\left(2\xi\frac{\partial f}{\partial\xi}+f\right), \tag{2.14}$$

equations (2.7)–(2.10) become

$$2\xi\frac{\partial F}{\partial\xi}+\frac{\partial V}{\partial\eta}+F=0 \tag{2.15}$$

$$2\xi F\frac{\partial F}{\partial\xi}+V\frac{\partial F}{\partial\eta}=(1+N_1)\frac{\partial^2F}{\partial\eta^2}+N_1\frac{\partial G}{\partial\eta^2}+2\xi\,\mathrm{Gr}\,\theta \tag{2.16}$$

$$N_2\left(2\xi F\frac{\partial G}{\partial\xi}+V\frac{\partial G}{\partial\eta}-GF\right)=N_3\frac{\partial^2G}{\partial\eta^2}-2N_1\xi\left(\frac{\partial F}{\partial\eta}+2G\right) \tag{2.17}$$

$$2\xi F\frac{\partial\theta}{\partial\xi}+V\frac{\partial\theta}{\partial\eta}=\frac{1}{\mathrm{Pr}}\frac{\partial^2\theta}{\partial\eta^2}. \tag{2.18}$$

The boundary conditions are

$$\begin{aligned} &\eta=0\text{: } F=0,\ V=0,\ G=0,\ \theta=1,\\ &\eta\to\infty\text{: } F\to1,\ G\to0,\ \theta\to0. \end{aligned} \tag{2.19}$$

Transformation to finite domain

The system of partial differential equations (2.15)–(2.18), which involves two independent variables ξ and η, both varying from 0 to ∞, is to be solved for V, F, G and θ with the use of finite difference formulae. In order to facilitate the application of finite-difference schemes, we transform the equations to a new system of coordinates wherein the indefinite limit of integration in η is replaced by a definite limit. Employing the transformation

$$Y=1-\mathrm{e}^{-a\eta},$$

where α is a constant, satisfying $\alpha > 0$, that can be used as a scaling factor to provide an optimum distribution at nodal points across the boundary layer, we arrive at the following set of equations for V, F, G and θ:

$$2\xi\frac{\partial F}{\partial \xi} + Y'\frac{\partial V}{\partial Y} + F = 0, \tag{2.20}$$

$$2\xi F\frac{\partial F}{\partial \xi} + Y'V\frac{\partial F}{\partial Y} = (1+N_1)\left[Y''\frac{\partial F}{\partial Y} + Y'^2\frac{\partial^2 F}{\partial Y^2}\right] + N_1 Y'\frac{\partial G}{\partial Y} + 2\xi\,\mathrm{Gr}\,\theta \tag{2.21}$$

$$N_2\left(2\xi F\frac{\partial G}{\partial \xi} + Y'V\frac{\partial G}{\partial Y} - GF\right) = N_3\left(Y''\frac{\partial G}{\partial Y} + Y'^2\frac{\partial^2 G}{\partial Y^2}\right) - 2N_1\xi\left(Y'\frac{\partial F}{\partial Y} + 2G\right) \tag{2.22}$$

$$2\xi F\frac{\partial \theta}{\partial \xi} + Y'V\frac{\partial \theta}{\partial Y} = \frac{1}{\mathrm{Pr}}\left(Y''\frac{\partial \theta}{\partial Y} + Y'^2\frac{\partial^2 \theta}{\partial Y^2}\right). \tag{2.23}$$

where a prime denotes differentiation with respect to η. The boundary conditions (2.19) now become

$$\begin{aligned} &Y = 0\text{: } F = 0,\ V = 0,\ G = 0,\ \theta = 1,\\ &Y = 1\text{: } F = 1,\ G = 0,\ \theta = 0. \end{aligned} \tag{2.24}$$

To complete the governing equations, initial conditions are obtained at $\xi = 0$ from equations (2.20)–(2.23), which become ordinary differential equations at $\xi = 0$. These equations are

$$Y'\frac{\mathrm{d}V}{\mathrm{d}Y} + F = 0 \tag{2.25}$$

$$Y'V\frac{\mathrm{d}F}{\mathrm{d}Y} - (1+N_1)\left[Y''\frac{\mathrm{d}F}{\mathrm{d}Y} + Y'^2\frac{\mathrm{d}^2 F}{\mathrm{d}Y^2}\right] - N_1 Y'\frac{\mathrm{d}G}{\mathrm{d}Y} = 0 \tag{2.26}$$

$$N_2\left(Y'V\frac{\mathrm{d}G}{\mathrm{d}Y} - GF\right) - N_3\left(Y''\frac{\mathrm{d}G}{\mathrm{d}Y} + Y'^2\frac{\mathrm{d}^2 G}{\mathrm{d}Y^2}\right) = 0 \tag{2.27}$$

$$Y'V\frac{\mathrm{d}\theta}{\mathrm{d}Y} - \frac{1}{\mathrm{Pr}}\left(Y''\frac{\mathrm{d}\theta}{\mathrm{d}Y} + Y'^2\frac{\mathrm{d}^2 G}{\mathrm{d}Y^2}\right) = 0. \tag{2.28}$$

The boundary conditions for equations (2.25)–(2.28) are the same as given in (2.24).

Skin-friction coefficient

The skin-friction coefficient C_f is defined by

$$C_f = \frac{(t_{yx})_{y=0}}{\rho U_\infty{}^2} = \left(\frac{1}{\rho U_\infty{}^2}\right)\left[(\mu_r + K_r)\frac{\partial u}{\partial y} + K_r v\right]_{y=0}$$

$$= \frac{\mu_r + K_r}{\rho U_\infty{}^2}\left(\frac{\partial u}{\partial y}\right)_{y=0},$$

since $v = 0$ at $y = 0$.

In terms of the non-dimensional quantities (2.6) and the variables given in (2.12)–(2.14), after dropping the asterisks, we have

$$C_f = \left[(1+N_1)\frac{\partial u}{\partial y}\right]_{y=0} = \frac{(1+N_1)}{\sqrt{2\xi}}\left(\frac{\partial F}{\partial \eta}\right)_{\eta=0}. \tag{2.29a}$$

In transformed coordinate (for finite domain), we have

$$C_f = \frac{\alpha(1+N_1)}{\sqrt{2\xi}}\left(\frac{\partial F}{\partial Y}\right)_{Y=0}. \tag{2.29b}$$

Heat transfer coefficient

The non-dimensional heat transfer coefficient called Nusselt number $N(x)$ is defined as

$$N(x) = \frac{q_y(\mu_v/\rho U_\infty)}{k_c(T_w - T_\infty)},$$

where q_y is the heat flux at the wall and defined as

$$q_y = \left(k_c\frac{\partial T}{\partial y} + \beta_c\frac{\partial v}{\partial x}\right)_{y=0} = k_c\left(\frac{\partial T}{\partial y}\right)_{y=0},$$

in view of $v = 0$ at $y = 0$. (β_c is the micropolar heat conduction coefficient).

Making use of the non-dimensional quantities (2.6), the Nusselt number (after dropping the asterisks) is given by

$$N(x) = \left(\frac{\partial\theta}{\partial y}\right)_{y=0}.$$

In terms of the variables given in (2.12)–(2.14), we have

$$N(\xi) = \frac{1}{\sqrt{2\xi}}\left(\frac{\partial\theta}{\partial\eta}\right)_{\eta=0}. \tag{2.30a}$$

In transformed coordinate (for finite domain), we have

$$N(\xi) = \frac{\alpha}{\sqrt{2\xi}}\left(\frac{\partial\theta}{\partial Y}\right)_{Y=0}. \tag{2.30b}$$

3. METHOD OF SOLUTION

A numerical solution of (2.20)–(2.23) subject to the initial conditions (2.25)–(2.28) and the boundary conditions (2.24) may be obtained by converting them into a set of implicit finite-difference equations of the Crank–Nicholson type. The mesh-point diagram for the Crank–Nicholson scheme is shown in Fig. 1. Suppose that there are $N+1$ nodal points in the Y direction then we have $N(\Delta Y) = 1$.

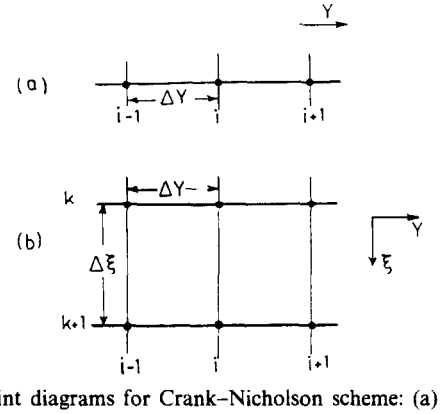

Fig. 1. Mesh-point diagrams for Crank–Nicholson scheme: (a) $\xi = 0$; (b) $\xi \neq 0$.

(a) *Solution for initial conditions*

We solve equations (2.25)–(2.28) along with the boundary conditions (2.24) using finite-difference technique. We decouple these equations and adopt iterative process to solve each equation separately for a single dependent variable. As for example, we first solve (2.26) for F assuming linear profiles for V and G to start with across the boundary layer. In (2.26), we replace the derivatives in terms of central differences, e.g.

$$\frac{dF}{dY}=\frac{F_{i+1}-F_{i-1}}{2\Delta Y},\quad \frac{d^2F}{dY^2}=\frac{F_{i+1}-2F_i+F_{i-1}}{(\Delta Y)^2}.$$

The difference equation for F is now of the form

$$A_iF_{i-1}+B_iF_i+C_iF_{i+1}=D_i,\quad i=2,\ldots,N, \tag{3.1}$$

where

$$A_i=-\frac{V_iY_i'}{2\Delta Y}+\frac{(1+N_1)Y_i''}{2\Delta Y}-\frac{(1+N_1)Y_i'^2}{(\Delta Y)^2},$$

$$B_i=\frac{2(1+N_1)Y_i'^2}{(\Delta Y)^2},$$

$$C_i=\frac{V_iY_i'}{2\Delta Y}-\frac{(1+N_1)Y_i''}{2\Delta Y}-\frac{(1+N_1)Y_i'^2}{(\Delta Y)^2},$$

$$D_i=\frac{N_1(G_{i+1}-G_{i-1})Y_i'}{2\Delta Y}.$$

We solve this linear system of algebraic equations using Thomas algorithm[19].

Similarly, we solve equation (2.27) for G and equation (2.28) for θ. After this, we solve equation (2.25) for V by writing in the form

$$V_i=-\int_0^Y F_i/Y_i'\,dY. \tag{3.2}$$

Using trapezoidal rule we evaluate the integral on the r.h.s. of (3.2). The new values thus obtained are used again in (3.1) for next iteration and so on. This cycle of computation is repeated till convergence is achieved, i.e. the difference between the two successive iterates of each dependent variable is less than preassigned tolerance, say 10^{-4}.

(b) *Solution of equations* (2.20)–(2.23)

We have decoupled equations (2.20)–(2.23) and solved each equation separately for a single dependent variable at each station. Equation (2.21) is solved for F, (2.22) for G, (2.23) for θ and (2.20) for V in that order. We replace, in each equation, the derivatives with respect to Y in terms of central differences, and with respect to ξ in terms of forward differences. For example, we have used the following type of finite-difference equations to approximate the unknowns and their derivatives in (2.21):

$$\xi=\frac{1}{2}(\xi_k+\xi_{k+1}),\ \frac{\partial F}{\partial\xi}=(F_{i,k+1}-F_{i,k})/\Delta\xi,$$

$$\frac{\partial F}{\partial Y}=(F_{i+1,k}-F_{i-1,k}+F_{i+1,k+1}-F_{i-1,k+1})/(4\Delta Y),$$

$$\frac{\partial^2F}{\partial Y^2}=(F_{i+1,k}-2F_{i,k}+F_{i-1,k}+F_{i+1,k+1}-2F_{i,k+1}+F_{i-1,k+1})/[2(\Delta Y)^2].$$

Further, we have used the following finite-difference equations for linearization of (2.21):

$$\frac{\partial G}{\partial Y} = (G_{i+1,k} - G_{i-1,k})/(2\Delta Y), \quad F = F_{i,k}, \quad V = V_{i,k}, \quad \theta = \theta_{i,k}.$$

After substituting these expressions, the difference equation for F at $(k+1)$th station is of the form

$$A_{i,k}F_{i-1,k+1} + B_{i,k}F_{i,k+1} + C_{i,k}F_{i+1,k+1} = D_{i,k}, \quad i = 2, \ldots, N, \tag{3.3}$$

where

$$A_{i,k} = -\frac{V_{i,k}Y_i'}{4\Delta Y} + \frac{(1+N_1)Y_i''}{4\Delta Y} - \frac{(1+N_1)Y_i'^2}{2(\Delta Y)^2},$$

$$B_{i,k} = \frac{F_{i,k}(\xi_k + \xi_{k+1})}{\Delta\xi} + \frac{(1+N_1)Y_i'^2}{(\Delta Y)^2},$$

$$C_{i,k} = \frac{V_{i,k}Y_i'}{4\Delta Y} - \frac{(1+N_1)Y_i''}{4\Delta Y} - \frac{(1+N_1)Y_i'^2}{2(\Delta Y)^2},$$

$$D_{i,k} = \frac{F_{i,k}^2(\xi_k + \xi_{k+1})}{\Delta\xi} - \frac{V_{i,k}(F_{i+1,k} - F_{i-1,k})Y_i'}{4\Delta Y}$$

$$+ (1+N_1)\left[\frac{(F_{i+1,k} - F_{i-1,k})Y_i''}{4\Delta Y} + \frac{(F_{i+1,k} - 2F_{i,k} + F_{i-1,k})Y_i'^2}{2(\Delta Y)^2}\right]$$

$$+ \frac{N_1(G_{i+1,k} - G_{i-1,k})Y_i'}{2\Delta Y} + \mathrm{Gr}(\xi_k + \xi_{k+1})\theta_{i,k}.$$

The functions V, G and θ appearing in the coefficients $A_{i,k}$, $B_{i,k}$, $C_{i,k}$ and $D_{i,k}$ are taken to be known from the initial conditions or from the values at previous station as the case may be. This amounts to solving the algebraic system of equations (3.3) for F alone. This system of equations for F is solved by using Thomas algorithm[19].

Proceeding in a similar manner, as outlined above for the dependent variable F, we obtain the solutions of the systems of linear algebraic equations for G and θ wherein the functions appearing in the coefficients of the algebraic equations have been appropriately averaged. In order to preserve the brevity of the analysis we are not giving further details. These details are available in [20].

The functions and derivatives in continuity equation (2.20) are approximated with the following finite-difference relations:

$$\xi = \frac{1}{2}(\xi_k + \xi_{k+1}), \quad F = \frac{1}{4}(F_{i,k} + F_{i+1,k} + F_{i,k+1} + F_{i+1,k+1}),$$

$$\frac{\partial F}{\partial \xi} = (F_{i,k+1} - F_{i,k} + F_{i+1,k+1} - F_{i+1,k})/(2\Delta\xi),$$

$$\frac{\partial V}{\partial Y} = (V_{i+1,k} - V_{i,k} + V_{i+1,k+1} - V_{i,k+1})/(2\Delta Y).$$

The resulting relation is

$$V_{i+1,k+1} = \left[\left(-\frac{1}{2\Delta\xi}\right)(\xi_k + \xi_{k+1})(F_{i,k+1} - F_{i,k} + F_{i+1,k+1} - F_{i+1,k})\right.$$

$$\left. - \left(\frac{1}{4}\right)(F_{i,k} + F_{i+1,k} + F_{i,k+1} + F_{i+1,k+1})\right] \Big/ \left(\frac{2\Delta Y}{Y_i'}\right)$$

$$- V_{i+1,k} + V_{i,k} + V_{i,k+1}, \quad i = 1, \ldots, N. \tag{3.4}$$

The new values thus obtained from (3.4) for V are used in (3.3) for next station and so on.

This cycle of computation for all the dependent variables is repeated till the convergence for this computational scheme is achieved. The criterion for whether the convergence has been achieved or not is that the difference between the values of each dependent variable at two successive stations is less than 10^{-4}.

Skin-friction and heat transfer

The velocity gradient and temperature gradient on the surface used in the expressions for skin-friction coefficient (2.29) and heat transfer coefficient (2.30), respectively, are determined from the following second-order expressions

$$\left(\frac{\partial F}{\partial \eta}\right)_{\eta=0} = \left(Y' \frac{\partial F}{\partial Y}\right)_{Y=0} = \left(\frac{\alpha}{\Delta Y}\right)[-(3/2)F_1 + 2F_2 - (1/2)F_3] \tag{3.5}$$

$$\left(\frac{\partial \theta}{\partial \eta}\right)_{\eta=0} = \left(\frac{\alpha}{\Delta Y}\right)[-(3/2)\theta_1 + 2\theta_2 - (1/2)\theta_3]. \tag{3.6}$$

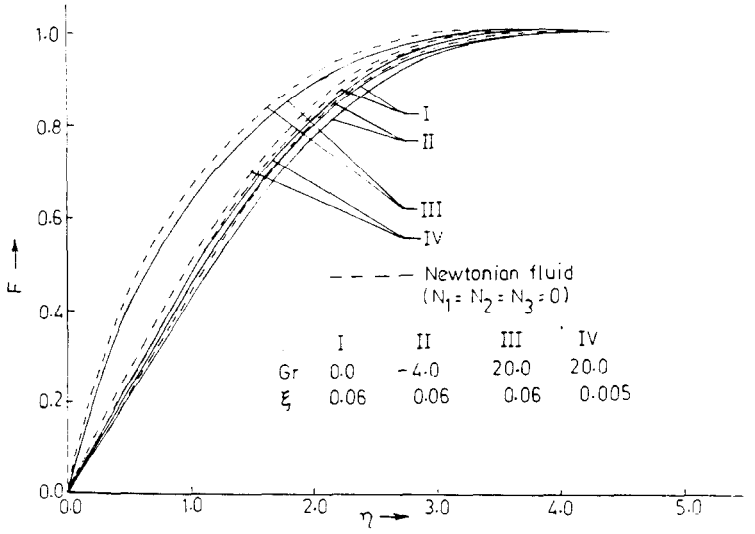

Fig. 2(a). Velocity distribution: $N_1 = 0.1$; $N_2 = 0.002$; $N_3 = 0.02$, Pr = 9.0.

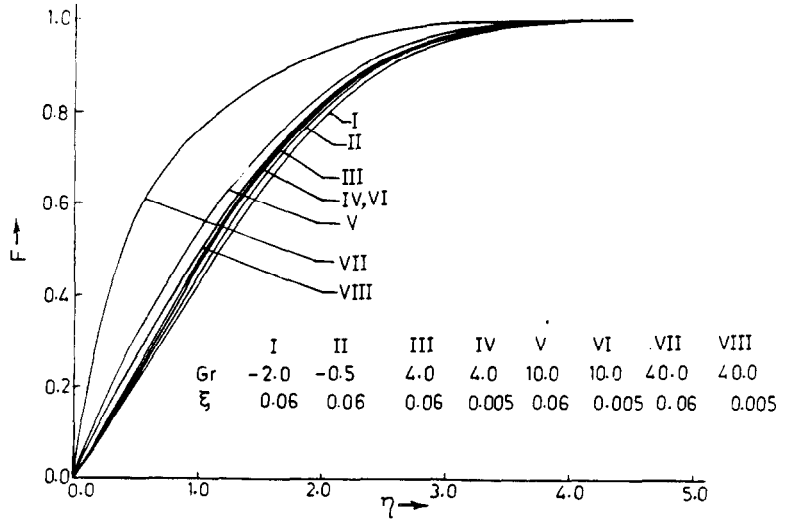

Fig. 2(b). Velocity distribution; $N_1 = 0.1$; $N_2 = 0.002$; $N_3 = 0.02$; Pr = 9.0

4. RESULTS AND DISCUSSION

It is worth mentioning that the problem under consideration is having a free stream temperature T_∞ and the body temperature is T_w. Hence, it is pertinent to enquire the effect of these temperatures on the flow field. For if $T_w > T_\infty$, the free convection currents will flow from the plate to the free stream and hence the plate loses heat, as a result of this the fluid is being heated. In otherwords, it is termed as cooling of the plate when $T_w - T_\infty > 0$, i.e. $\mathrm{Gr} > 0$. Conversely, if $T_w - T_\infty < 0$, i.e. $\mathrm{Gr} < 0$, the free convection currents travel from the free stream to the plate and this case corresponds to heating of the plate (cooling of the fluid) by free convection currents. When $T_w = T_\infty$, i.e. $\mathrm{Gr} = 0$, the plate temperature equals the free stream temperature and the flow is solely due to forced convection.

In carrying out the numerical calculations, we have assigned various values to Gr as recorded on Figs. 2–4 and Tables 1 and 2. Further, we have chosen the following values for the other parameters:

$$N_1 = 0.1,\ N_2 = 0.002,\ N_3 = 0.02,\ \alpha = 0.5,\ \mathrm{Pr} = 9.0.$$

This set of values of the non-dimensional parameters have been chosen keeping in view the thermodynamic restrictions on the material parameters mentioned by Eringen[7–9]. We have chosen only one set of values of the parameters because the effect of the variation of the material parameters N_1, N_2 and N_3 has already been studied in detail in Refs. [13] and [20] for different flow problems of micropolar fluids involving free convection. Throughout the computations, we have taken $\Delta\xi = 0.005$ and $\Delta Y = 0.001$. The numerical solutions have been obtained by the use of DEC-10 computer.

Velocity field

The velocity profiles have been plotted in Figs. 2(a) and (b) at different stations to show the effect of variation of Gr on velocity field. From Figs. 2(a) and (b), we observe that the velocity increases with increasing positive values of Gr which is due to more heating of the fluid. The velocity decreases as Gr goes from (-0.5) to (-4.0) due to more cooling of the fluid. Further, we observe that for a large value of Gr, in the case of fluid-heating velocity increases with the increases of ξ. On the other hand, velocity decreases with the increase of ξ in both cases of fluid-cooling and of purely forced flow. However, this decrease in velocity is extremely small. Therefore, we do not present graphically the variation of the flow for different values of ξ for $\mathrm{Gr} < 0$ and $\mathrm{Gr} = 0$. The profiles in Fig. 2(a) are compared with the corresponding profiles for a Newtonian fluid shown with broken lines. From Fig. 2(a), we see that the velocity for a micropolar fluid is always less

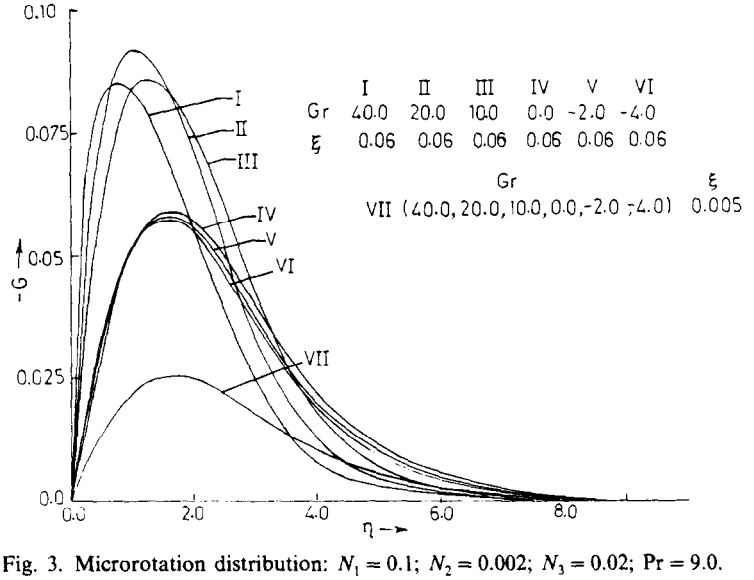

Fig. 3. Microrotation distribution: $N_1 = 0.1$; $N_2 = 0.002$; $N_3 = 0.02$; $\mathrm{Pr} = 9.0$.

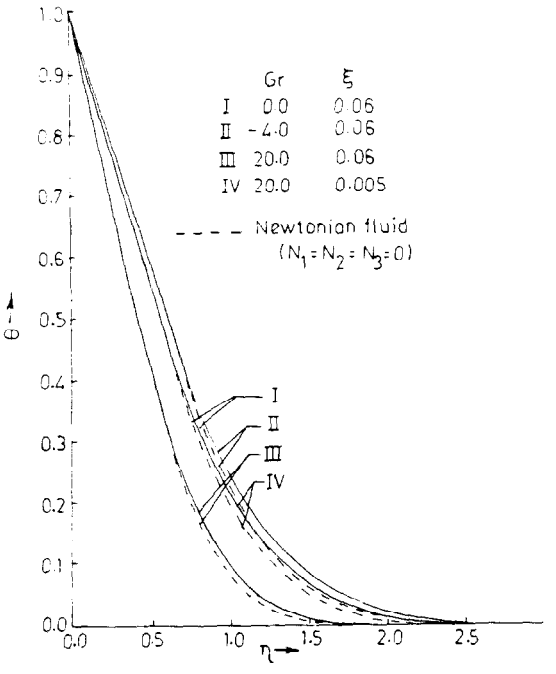

Fig. 4(a). Temperature distribution: $N_1 = 0.1$; $N_2 = 0.002$; $N_3 = 0.02$; Pr = 9.0.

than that of a Newtonian fluid. This is due to the fact that the micropolar fluids offer greater resistance to the fluid motion in comparison to a Newtonian fluid. The results presented in Fig. 2(b) have also been compared with the corresponding results for a Newtonian fluid but we have not shown this comparison in Fig. 2(b) because it does not differ qualitatively from what has been presented in Fig. 2(a).

Microrotation field

Figure 3 depicts the behaviour of microrotation for various values of Gr. We observe that the microrotation is very sensitive to the changes in values of Gr when fluid is being

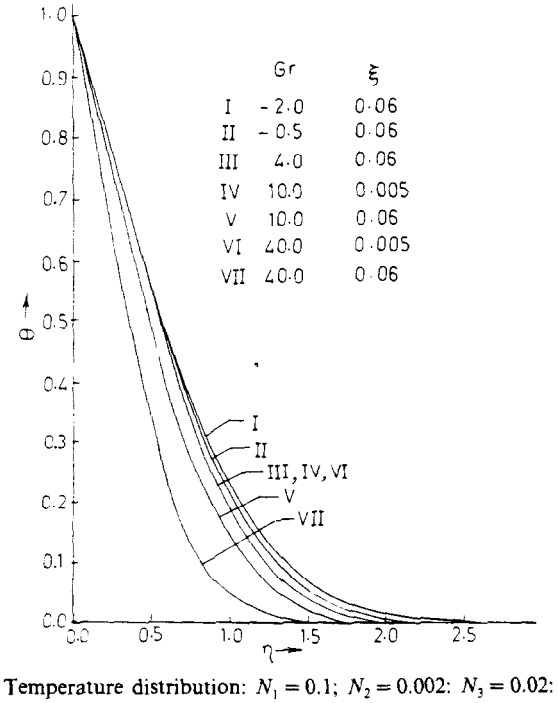

Fig. 4(b). Temperature distribution: $N_1 = 0.1$; $N_2 = 0.002$: $N_3 = 0.02$: Pr = 9.0.

Table 1. Skin-friction parameter, $(\partial F/\partial \eta)_{\eta=0}$, with $\Delta\xi = 0.005$, $\Delta Y = 0.001$ and $\alpha = 0.5$

	Gr							
ξ	40.0	20.0	10.0	4.0	0.0	−0.5	−2.0	−4.0
	Micropolar fluid ($N_1 = 0.1$, $N_2 = 0.002$, $N_3 = 0.02$, Pr = 9.0)							
0.005	0.5997	0.5236	0.4855	0.4627	0.4475	0.4456	0.4399	0.4323
0.02	1.0796	0.7860	0.6230	0.5010	0.4460	0.4390	0.4180	0.3898
0.04	1.5583	1.0660	0.7439	0.5855	0.4451	0.4381	0.4162	0.3887
0.06	1.9805	1.1933	0.7558	0.6032	0.4435	0.4375	0.4151	0.3875
0.1	2.0032	1.2005	0.7589	0.6112	0.4430	0.4370	0.4144	0.3855
	Newtonian fluid ($N_1 = N_2 = N_3 = 0.0$, Pr = 9.0)							
0.05	0.6325	0.5509	0.5101	0.4857	0.4694	0.4673	0.4612	0.4530
0.02	1.1505	0.8363	0.6620	0.5498	0.4675	0.4636	0.4412	0.4110
0.04	1.6635	1.1373	0.7928	0.5921	0.4652	0.4662	0.4408	0.4005
0.06	2.1156	1.2741	0.7931	0.6508	0.4635	0.4609	0.4397	0.4000
0.1	2.1175	1.2755	0.7935	0.6519	0.4621	0.4600	0.4389	0.3996

Table 2. Rate of heat transfer parameter, $[-(\partial\theta/\partial\eta)_{\eta=0}]$ with $\Delta\xi = 0.005$, $\Delta Y = 0.001$ and $\alpha = 0.5$

	Gr							
ξ	40.0	20.0	10.0	4.0	0.0	−0.5	−2.0	−4.0
	Micropolar fluid ($N_1 = 0.1$, $N_2 = 0.002$, $N_3 = 0.02$, Pr = 9.0)							
0.005	0.9635	0.9626	0.9621	0.9619	0.9617	0.9616	0.9616	0.9615
0.02	1.1781	1.0738	1.0070	0.9630	0.9307	0.9278	0.9191	0.9071
0.04	1.3404	1.1955	1.0724	0.9955	0.9300	0.9272	0.9180	0.9066
0.06	1.4590	1.2434	1.0988	1.0005	0.9285	0.9269	0.9006	0.8905
0.1	1.4598	1.2752	1.1005	1.0018	0.9277	0.9265	0.9001	0.8900
	Newtonian fluid ($N_1 = N_2 = N_3 = 0$, Pr = 9.0)							
0.005	0.9776	0.9767	0.9762	0.9760	0.9758	0.9757	0.9757	0.9756
0.02	1.1998	1.0932	1.0248	0.9764	0.9472	0.9443	0.9353	0.9231
0.04	1.3664	1.2183	1.0933	0.9967	0.9425	0.9412	0.9340	0.9213
0.06	1.4875	1.2673	1.0995	1.0021	0.9402	0.9380	0.9321	0.9201
0.1	1.4882	1.2677	1.1007	1.0023	0.9383	0.9367	0.9302	0.9187

heated by the free convection current ($T_w > T_\infty$) while it is rather insensitive when fluid is being cooled by the free convection current. It is interesting to note from Fig. 3 that microrotation near the leading edge of the plate ($\xi = 0.005$) is affected nominally by Grashof number Gr and these changes are too small to be shown graphically. Furthermore, it seems from Fig. 3 that there exists a contact layer when fluid is heated more strongly. It may be mentioned here that for $N_3 \to 0$, that is for vanishing microdiffusivity, similar phenomenon, as shown in Fig. 3, on microrotation, was observed by Willson[21] who calls it as a contact layer. We notice from Fig. 3 that these profiles cross each other in the fluid heating case. Similar profiles for microrotation were also obtained by Kümmerer[22].

Temperature field

Some representative temperature profiles are given in Figs. 4(a) and (b). The broken lines in Fig. 4(a) indicate the corresponding curves for a Newtonian fluid. It is clear from Figs. 4(a) and (b) that the temperature decreases as Gr increases for cooling of the plate (Gr > 0) and vice-versa for heating of the plate (Gr < 0). Purely force convection results, which corresponds to Gr = 0, are plotted in Fig. 4(a) for comparison. For the same reason as in the case of velocity field we compare the results for the corresponding results of a Newtonian fluid only for a few selected values of Gr. These profiles show that there is a definite effect of microrotation as compared to Newtonian fluids. It is observed from Figs. 4(a) and (b) that the effect of the changes in values of Gr on temperature is more pronounced for $\xi = 0.06$.

The skin-friction parameter has been tabulated in Table 1. We note that skin-friction decreases with the decrease of Grashof number Gr. Further, we observed that in the case

of heating of the fluid ($Gr > 0$) skin-friction increases, for a fixed value of Gr with the increase of ξ. Skin-friction decreases with the increase of ξ in the case of fluid-cooling ($Gr < 0$) as well as in purely forced flow ($Gr = 0$). The above noticed phenomenon is also observed for Newtonian fluids (Table 1). In comparison to a Newtonian fluid, the skin-friction is reduced for a miropolar fluid.

In Table 2, we have recorded the values of the rate of heat transfer parameter (gradient of temperature) on the plate. We observe that $[-(\partial\theta/\partial\eta)_{\eta=0}]$ decreases with the decreasing Gr. Furthermore, we notice from Table 2 that $[-(\partial\theta/\partial\eta)_{\eta=0}]$ increases with the increasing ξ for fluid-heating case ($Gr > 0$) but the opposite happens in the case of fluid-cooling ($Gr < 0$) as well as forced flow ($Gr = 0$). Corresponding results for a Newtonian fluid have been recorded in Table 2.

We have already seen from Figs. 4(a) and (b) that the temperature of a micropolar fluid is more than that of a Newtonian fluid. This can be explained as follows:

The temperature distribution $\theta(\xi, \eta)$ at any point (ξ, η) inside the boundary layer at a small distance 'd' from the plate can be approximately written as

$$\theta(\xi, \eta) = \theta(\xi, 0) + d\theta'(\xi, 0),$$

where $\theta'(\xi, 0) = (\partial\theta/\partial\eta)_{\eta=0}$.

The difference between the temperature of a Newtonian fluid and a micropolar fluid at the same point inside the boundary layer can be written as

$$[\theta(\xi, \eta)]_{\text{Newtonian}} - [\theta(\xi, \eta)]_{\text{Micropolar}} = d\{[\theta'(\xi, 0)]_{\text{Newtonian}} - [\theta'(\xi, 0)]_{\text{Micropolar}}\}. \quad (4.1)$$

Since $\theta'(\xi, 0)$ is negative, and its absolute value is greater for a Newtonian fluid than that for a micropolar fluid (Table 2), the temperature of a Newtonian fluid is less than the temperature of a micropolar fluid in view of the relation (4.1).

Acknowledgement—One of the authors (S.K.J.) wishes to thank the Council of Scientific and Industrial Research, Government of India, for the financial assistance.

REFERENCES

1. J. R. Lloyd and E. M. Sparrow, Combined forced and free convection flow on vertical surface. *Int. J. Heat Mass Transfer* **13**, 434–438 (1970).
2. G. Wilks, Combined forced and free convection flow on vertical surfaces. *Int. J. Heat Mass Transfer* **16**, 1958–1964 (1973).
3. P. H. Oosthuizen and R. Hart, A numerical study of laminar combined convective flow over flat plates. *J. Heat Transfer, Trans. ASME* **95**, 60–63 (1973).
4. J. Gryzagoridis, Combined free and forced convection from an isothermal vertical plate. *Int. J. Heat Mass Transfer.* **18**, 911–916 (1975).
5. K. A. Kline and S. J. Allen, Heat conduction in fluids with substructure. *ZAMM* **48**, 435–438 (1968).
6. T. Ariman, M. A. Turk and N. D. Sylvester, Microcontinuum fluid mechanics—a review. *Int. J. Engng Sci.* **11**, 905–930 (1973).
7. A. C. Eringen, Theory of micropolar fluids. *J. Math. Mech.* **16**, 1–18 (1966).
8. A. C. Eringen, Mechanics of micropolar continua. *Contribution to Mechanics* (Edited by D. Abir), pp. 23–40. Pergamon Press, Oxford (1970).
9. A. C. Eringen, Theory of thermomicrofluids. *J. Math. Anal. Appl.* **38**, 480–496 (1972).
10. M. Balaram and V. U. K. Sastry, Micropolar free convection flow. *Int. J. Heat Mass Transfer* **16**, 437–441 (1973).
11. G. Maiti, Convective heat transfer in micropolar fluid flow through a horizontal parallel plate channel. *ZAMM* **55**, 105–111 (1975).
12. V. U. K. Sastry and G. Maiti, Numerical solution of combined convective heat transfer of micropolar fluid in an annulus of two vertical pipes. *Int. J. Heat Mass Transfer* **19**, 207–211 (1976).
13. S. K. Jena and M. N. Mathur, Similarity solutions for laminar free convection flow of a thermomicropolar fluid past a nonisothermal vertical flat plate. *Int. J. Engng Sci.* **19**, 1431–1439 (1981).
14. J. A. Sills, Transformations for infinite regions and their applications to flow problems. *AIAA J.* **7**, 117–123 (1969).
15. P. S. Ramachandran, M. N. Mathur and S. K. Ojha, Heat transfer in boundary layer flow of a micropolar fluid past a curved surface with suction and injection. *Int. J. Engng Sci.* **17**, 625–639 (1979).
16. M. N. Mathur, S. K. Ojha and P. S. Ramachandran, Thermal boundary layer of a micropolar fluid on a circular cylinder. *Int. J. Heat Mass Transfer* **21**, 923–933 (1978).
17. G. Ahmadi, Stability of a micropolar fluid layer heated from below, *Int. J. Engng Sci.* **14**, 81–89 (1976).
18. R. S. R. Gorla, Thermal boundary layer of a micropolar fluid at a stagnation point. *Int. J. Engng Sci.* **18**, 611–617 (1980).

19. W. F. Ames, *Numerical Methods for Partial Differential Equations*, pp. 49–54. Thomas Nelson, London (1969).
20. S. K. Jena, Convective heat transfer and stability of thermomicropolar fluids. Ph.D. Thesis, Indian Institute of Technology, Bombay (1983).
21. A. J. Willson, Boundary layers in micropolar fluids, *Proc. Camb. Phil. Soc.* **67**, 469–476 (1970).
22. H. Kümmerer, Similar laminar boundary layers in incompressible micropolar fluids. *Rheol. Acta* **16**, 261–265 (1977).